Magnetic anisotropy of $L1_0$ FePt and $Fe_{1-x}Mn_xPt$

Till Burkert,[1,*] Olle Eriksson,[1,4] Sergei I. Simak,[1,2] Andrei V. Ruban,[3] Biplab Sanyal,[1] Lars Nordström,[1] and John M. Wills[4]
[1]*Department of Physics, Uppsala Universitet, Box 530, 751 21 Uppsala, Sweden*
[2]*Department of Physics and Measurement Technology, Linköping University, 581 83 Linköping, Sweden*
[3]*Department of Material Science and Engineering, Royal Institute of Technology (KTH), 100 44 Stockholm, Sweden*
[4]*Theoretical Division, Los Alamos National Laboratory, Los Alamos, New Mexico 87545, USA*
(Received 24 August 2004; revised manuscript received 22 November 2004; published 14 April 2005)

The uniaxial magnetic anisotropy energy (MAE) of $L1_0$ FePt and $Fe_{1-x}Mn_xPt$, $x=0-0.25$, was studied from first principles using two fully relativistic computational methods, the full-potential linear muffin-tin orbitals method and the exact muffin-tin orbitals method. It was found that the large MAE of 2.8 meV/f.u. is caused by a delicate interaction between the Fe and Pt atoms, where the large spin-orbit coupling of the Pt site and the hybridization between Fe 3*d* and Pt 5*d* states is crucial. The effect of random order on the MAE was modeled by mutual alloying of the sublattices within the coherent potential approximation (CPA), and a strong dependence of the MAE on the degree of chemical long-range order was found. The alloying of FePt with Mn was investigated with the virtual crystal approximation and the CPA as well as supercell calculations. The MAE increases up to 33% within the concentration range studied here, an effect that is attributed to band filling. Furthermore, the dependence of the MAE on the structural properties was studied.

DOI: 10.1103/PhysRevB.71.134411 PACS number(s): 75.30.Gw, 75.50.Bb, 75.50.Ss

I. INTRODUCTION

The interest in chemically ordered FePt stems from the large uniaxial magnetic anisotropy energy (MAE), of the order of meV/formula unit (f.u.), and a high Kerr rotation, making it a possible candidate for ultrahigh density magnetic and magneto-optical recording media.[1] Recently, FePt has been proposed as a building block of nanocomposite magnets.[2–6]

Chemically ordered FePt crystallizes in the $L1_0$ structure. It can be viewed as alternating atomic layers of Fe and Pt stacked along the [001] direction (*c* axis), which is also the magnetic easy axis. The chemically ordered phase can be prepared by annealing from the random state, or—as a thin film—by deposition at substrate temperatures above the $L1_0$ ordering temperature.[7–12] In a thin film, the orientation of the magnetic easy axis relative to the film plane is controlled by the substrate surface.[9] In that way, perpendicular magnetic anisotropy (PMA) can be obtained, which is desirable for magneto-optical recording applications.

Chemically ordered FePt and related compounds have been studied experimentally and theoretically by numerous authors. The purpose of this report is to investigate the MAE of FePt and its alloys with Mn. The focus is on the physical origin of the large MAE that is observed in FePt and its dependence on compositional order as well as structural properties, such as the c/a ratio. Several computational schemes have been used for these purposes.

The calculation of the MAE of the ferromagnetic transition metals and their compounds from first principles is not a trivial task. In the case of bcc Fe and fcc/hcp Co, e.g., the correct easy axes of magnetization are obtained—though underestimated in size—but not for fcc Ni.[13] For systems with a larger MAE, e.g., hcp Gd, and thin films and multilayers, the description is more successful.[14–20] In order to resolve the tiny energy differences of a material with the magnetization aligned in different directions, the integration in reciprocal space has to be performed with care. Apart from the convergence of the MAE with respect to the number of **k** points in the Brillouin zone (BZ), the details of the summation that is performed to obtain the band energy are of great importance, as different methods yield quantitatively different values for the MAE.[14,15] Furthermore, the choice of the approximation to the exchange correlation potential sometimes has a profound influence on the calculated MAE. Up to now it is not clear whether the local density approximation (LDA) or the generalized gradient approximation (GGA) should be used. According to Jansen[21] the incomplete description of the MAE is due to many-body correlations that are neglected in the LDA and GGA. Attempts have been made to include these effects that—apart from the spin-orbit coupling—give rise to enhanced orbital moments, into the density-functional theory. One scheme that has been proposed, the orbital polarization (OP) correction,[22] successfully describes the orbital moments of the ferromagnetic transition metals and their alloys.[13,23–25] The MAE, however, is usually overestimated in comparison to experiment.[13,19] In the case of FePt, the OP was found to have a negligible effect on the MAE.[17,26] A second route to recover the effect of the neglected many-body correlations is the LDA+U method.[27] In these calculations an additional parameter (or two, in the case of a binary alloy such as FePt), the so-called Hubbard *U*, is chosen to reproduce experimental results. It should be noted that the LDA reproduces the ground-state properties of elemental Pt as well as Pt-based compounds and alloys with good accuracy, and the use of an LDA+U approach with a finite *U* for the Pt site is difficult to motivate.

In the following the MAE is defined, in terms of the conventional $L1_0$ unit cell, as $\Delta E \equiv E^{100} - E^{001}$, where E^{100} and E^{001} are the total energies with the magnetization in the [100] and [001] directions, respectively. Thus, the MAE is defined to be positive if the easy axis is along the *c* axis.

II. COMPUTATIONAL DETAILS

Two different computational methods were used for the calculations presented here. Most of the calculations were done with a fully relativistic implementation of the full-potential linear muffin-tin orbitals (FP-LMTO) method.[28–30] The crystal is divided into nonoverlapping muffin-tin spheres centered around the atomic sites, with an interstitial region in between. For the expansion of the electron density and the potential inside the muffin-tins, spherical harmonics times a radial component are used. In the interstitial region the expansion makes use of a Fourier series. The basis functions are Bloch sums of Neumann and Hankel functions in the interstitial region that are augmented by a numerical basis function inside the muffin-tin spheres. The scalar-relativistic corrections were included in the calculation of the radial basis functions inside the muffin-tin spheres, whereas the spin-orbit coupling was included at the variational step, as described below.[28] A so-called double basis was used to ensure a well-converged wave function, i.e., two interstitial basis functions with different tail energies were used, each attached to its own (n,ℓ) radial function.

The MAE was evaluated from the force theorem, i.e., as the difference of the eigenvalue sums for the two magnetization directions.[31,32] First, the electron density was calculated self-consistently with a scalar-relativistic Hamiltonian, using the point-group symmetries that are common to both magnetization directions. Then, in a subsequent step, the eigenvalues were obtained by a single diagonalization for each magnetization direction, using the fully relativistic Hamiltonian and the scalar-relativistic self-consistent potential. To test the applicability of the force theorem in the present case, the MAE of FePt was calculated from total energies as well and was found to deviate by only 2.5% from the force theorem result.

For the calculation of the band energy two different methods were used. Most of the discussion in the remainder focuses on the results that were obtained with the modified tetrahedron method (MTM),[33] using 3.2×10^4 **k** points in the full Brillouin zone for $L1_0$ FePt, and correspondingly smaller amounts for the larger supercells that were used in the calculations of (Fe,Mn)Pt alloys. The advantage of the MTM is that it is exact in the limit of an infinite number of **k** points. For comparison, the BZ integration was performed with the special points method[34,35] as well, applying a Gaussian smearing to the eigenvalues close to the Fermi energy. The Gaussian broadening method (GBM) has been widely used for MAE calculations recently, but suffers from the fact that it might smear out details of the Fermi surface and yield a less accurate Fermi energy,[36] which may lead to an inaccurate MAE.[14] Its accuracy can be improved by using higher-order terms in the expansion of the δ function in Hermite polynomials[36] or correction terms.[37]

For the calculations of the (Fe,Mn)Pt alloys in the FP-LMTO method the virtual crystal approximation (VCA) was employed. In the VCA a binary alloy, in this case Fe and Mn, is modeled by a single atom with an effective atomic number $Z=(1-x)\cdot Z_{\mathrm{Fe}}+x\cdot Z_{\mathrm{Mn}}$, where $Z_{\mathrm{Fe}}=26$ and $Z_{\mathrm{Mn}}=25$, respectively. The VCA is expected to work well in the present case of a disordered alloy with constituents that have similar valence configurations.

In order to test the applicability of the VCA a fully relativistic implementation of the exact muffin-tin method (EMTO) was used.[38] It is a generalization of the Green's-function EMTO technique[39] for fully relativistic calculations. The spin-orbit coupling is treated in a nonperturbative way using a four-component Dirac equation. The EMTO calculations of the (Fe,Mn)Pt alloys were done with the coherent potential approximation (CPA), where the Mn atoms were assumed to be randomly distributed on the Fe sublattice, the situation that is encountered at experimental conditions.[40] The BZ integration was performed using a special point technique with about 2.5×10^4 **k** points in the full BZ and a Fermi-Dirac smearing. A Gaussian mesh of 16 energy points on a semicircle comprising the valence states was used for taking the energy integrals. For the EMTO method the MAE was calculated from total energies.

For the exchange-correlation potential the LDA was employed for most calculations. For comparison, the MAE of FePt was calculated with the GGA as well, and it was found to be 5% smaller compared to the LDA result. The OP correction was not applied, as its effect on the MAE of FePt is negligible.[17,26]

Different values for the equilibrium volume and the c/a ratio of $L1_0$ FePt have been published. The structure compiled by Villars,[41] $a=3.861$ Å and $c/a=0.981$ is the one most commonly used by other authors and was adopted here in order to facilitate comparison with previous theoretical studies.

III. RESULTS AND DISCUSSION

A. Brillouin zone integration

As the calculated MAE of many materials is crucially dependent on the details of the BZ integration, a closer look at the convergence of the MAE with respect to the number of **k** points, and the effect of different BZ integration techniques on the MAE, is needed. In Fig. 1 the uniaxial MAE of FePt, calculated in the experimental crystal structure, is shown for different **k** point sets and, for the FP-LMTO calculations, the two BZ integration techniques discussed in Sec. II. The calculations were done using the LDA for the exchange-correlation potential. For the GBM, two different smearing widths were used, 10 and 20 mRy. The simple Gaussian that is frequently used corresponds to the lowest-order term of an expansion of the δ function in Hermite polynomials.[36] Retaining higher-order terms is a possible route to improve on the accuracy, and the number of terms in the expansion N emerges as an additional convergence parameter. We used $N=0$, 1, and 2, where $N=0$ corresponds to a simple Gaussian smearing. From Fig. 1 it becomes obvious that the details of the BZ integration have a profound influence on the value of the calculated MAE. For a smearing of 10 mRy the GBM yields approximately the same result for the MAE as the MTM, irrespective of the value of N. Both methods show a similar convergence with respect to the number of **k** points. A larger smearing of 20 mRy, on the other hand, results in a stronger dependence of the MAE on the smearing function. Using a simple Gaussian smearing ($N=0$) results in a MAE that is 17% larger than that obtained from the MTM. For the

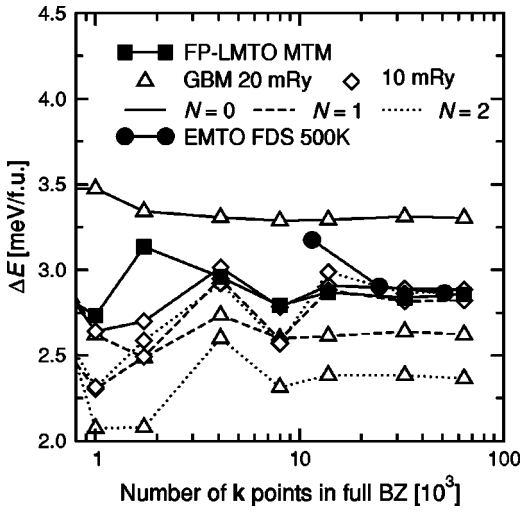

FIG. 1. Convergence of the MAE of $L1_0$ FePt, calculated with the FP-LMTO and EMTO methods, with respect to the number of **k** points in the full BZ. For the FP-LMTO method, the MAE was calculated with different BZ integration techniques.

results discussed in the remainder of the present paper the MTM was used for the FP-LMTO method. For the EMTO calculations a special point technique with a Fermi-Dirac smearing (FDS) of 500 K, was used (cf. Fig. 1). Calculations with other temperatures in the range 0–800 K gave similar results within 5%.

B. Compositional disorder

The uniaxial MAE of $L1_0$ FePt is usually overestimated by first-principles calculations, as compared to experimental studies.[7–9,11,12,49,50] In Table I the results of previous theoretical studies are compiled. Most of the theoretical values for the MAE are similar to the one reported here, around 2.6–2.8 meV/f.u. if the LDA is used. The largest experimental values reported in the literature, determined at room temperature, are 1.2 meV/f.u. for bulk,[49] and 1.1 meV/f.u. for thin films.[51] It was suggested that the discrepancy between the experimentally observed MAE and the theoretical studies, which amounts to a factor of 2–3, can be attributed to the absence of a perfect chemical order in the actual samples, which is assumed in most calculations, and/or the effect of temperature, as the experimental MAE is often determined at room temperature.[47,52] The correlation between the degree of chemical order and the MAE has been demonstrated experimentally by several authors.[7,8,51] To confirm this, we performed EMTO CPA calculations for different degrees of chemical long-range order, such that the Fe (Pt)

TABLE I. Calculated MAE of completely chemically ordered $L1_0$ FePt from previous theoretical studies. Abbreviations not appearing in the text: LAPW: linear augmented plane waves, ASW: augmented spherical waves, KKR: Korringa-Kohn-Rostoker.

Calc. method	approximations	BZ integration	c/a	MAE (meV/f.u.)	Ref.
FP-LMTO	LDA/GGA	MTM	0.981	2.84/2.71	present work
EMTO	LDA	FDS 500 K	0.981	2.86	present work
FP-LMTO	LDA/LDA+OP	GBM 10 mRy	0.981	2.73/2.89	Ravindran[a]
FP-LAPW	LDA/LDA+OP/LDA+U	GBM 1 mRy	0.98	2.68/2.9/1.3	Shick[b]
ASW	LDA	no smearing	0.957	2.75	Oppeneer[c]
LMTO-ASA	LDA	LTM	0.96	2.8	Sakuma[d]
LMTO-ASA	LDA/LDA+OP	LTM	0.96	3.3	Daalderop[e]
FP-LMTO	LDA/GGA	GBM 7 mRy	0.981	3.90/4.09	Galanakis[f]
KKR			0.981	1.8	Staunton[g]
KKR			0.981	4.3	Ostanin[h]
Real-space Green's-function technique			0.96	2.26	Solovyev[i]

[a]Reference 26
[b]Reference 42
[c]Reference 43
[d]Reference 44
[e]Reference 17
[f]Reference 45
[g]Reference 46
[h]Reference 47
[i]Reference 48

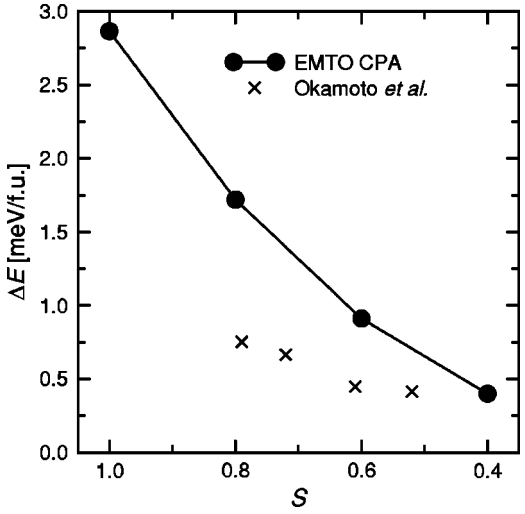

FIG. 2. Dependence of the MAE of FePt on the long-range order parameter *S*, calculated with the EMTO CPA method. The experimental results are from Okamoto *et al.*,[8] at 10 K.

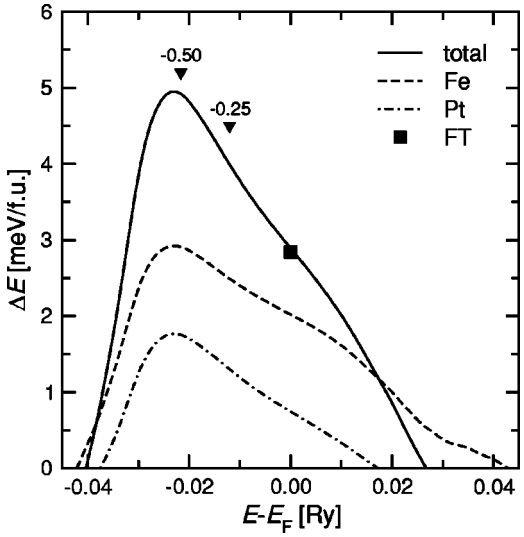

FIG. 3. Total and type-projected MAE of FePt as a function of the band filling. The closed square is the MAE obtained from the force theorem (FT). The position of the Fermi levels for valence electron states reduced by 0.25 and 0.5 electrons are marked by triangles. The contribution from the interstitial region is much smaller and was omitted.

sublattice is occupied by an $Fe_\eta Pt_{1-\eta}$($Pt_\eta Fe_{1-\eta}$) alloy, i.e., $\eta=1$ corresponds to complete order and $\eta=0.5$ to the random state. The long-range order parameter *S*, that can be determined experimentally, is related to the sublattice alloy concentration η by $S=2\eta-1$.[8–10,53,54] The dependence of the calculated MAE on *S* is shown in Fig. 2. It can be seen that the MAE is strongly dependent on the degree of chemical order. Even for highly ordered alloys, e.g., $S=0.9$,[8–10,53,54]—most of the experimental studies report order parameters <0.9—the MAE decreases in the calculations by 15–20%. Our findings are in agreement with those by Ostanin *et al.*[47] who concluded that the large MAE is mainly caused by the chemical order and that the tetragonal distortion of the fcc lattice plays only a minor role. Note that the volume and the c/a ratio were kept constant in these calculations. For the $L1_0$-ordered phase, the dependence of the MAE on the c/a ratio is discussed in Sec. III F. For comparison, the experimental result for the MAE of 140 Å thick FePt films[8] at 10 K is included in Fig. 2. Even if the quantitative agreement between the calculated and the measured MAE is far from satisfactory it becomes apparent that randomness has to be taken into account, in order to achieve a complete description of the MAE in first-principles calculations. The dependence of the MAE on the degree of chemical order was just recently studied by Staunton *et al.*[46] who obtain a qualitatively similar behavior, albeit with a smaller absolute value of the MAE that is in quantitative agreement with experiment.

C. Type-resolved MAE of FePt

To clarify the origin of the large MAE that is observed in $L1_0$ FePt we estimated the contribution from the different atomic types τ to the total MAE

$$\Delta E = \sum_{\tau=\mathrm{Fe,Pt}} \Delta E_\tau. \tag{1}$$

Following Ref. 55, ΔE_τ can be approximated as

$$\Delta E_\tau \approx F_\tau^{001}(\overline{E_F}) - F_\tau^{100}(\overline{E_F}), \tag{2}$$

where $\overline{E_F}$ is the average Fermi energy of the two magnetization directions σ, and $F_\tau^\sigma(E)$ can be calculated from the type-projected number of states $N_\tau^\sigma(E)$

$$F_\tau^\sigma(E) = \int_{-\infty}^{E} N_\tau^\sigma(\epsilon)\mathrm{d}\epsilon. \tag{3}$$

The result of this calculation, shown in Fig. 3, is that about 70% of the total MAE originates from the Fe atom. It should be noted that the value obtained from Eqs. (1)–(3) is in agreement with the MAE quoted in Table I, which was calculated from

$$\Delta E = \int_{-\infty}^{E_F^{100}} \epsilon D^{100}(\epsilon)\mathrm{d}\epsilon - \int_{-\infty}^{E_F^{001}} \epsilon D^{001}(\epsilon)\mathrm{d}\epsilon, \tag{4}$$

where D^σ is the density of states with the spin aligned along σ. The microscopic origin of the large MAE, however, can be attributed to the strong spin-orbit interaction of Pt in combination with hybridization between the Fe 3*d* and Pt 5*d* states. A calculation of the MAE of FePt with the spin-orbit coupling on the Pt site switched off yields a value of 0.41 meV/f.u., i.e., only 14% of the MAE calculated with the spin-orbit interaction included for both types of atoms. This conclusion is in agreement with a perturbation treatment of the orbital moment anisotropy (OMA),[48,56] which is connected to the microscopic origin of the MAE.[26,57] It was concluded that, in case of strong hybridization, the OMA can be enhanced by a strong spin-orbit coupling on ligand atoms.[56]

D. MAE of $Fe_{1-x}Mn_xPt$

The approach taken in the previous section allows us to estimate the dependence of the MAE on small variations of the actual band filling, both for the type-projected and for the total MAE. The latter can be calculated by using the total number of states in Eq. (3).

The dependence of the total MAE on band filling is shown in Fig. 3 and is in good agreement with the results by Sakuma.[44] Figure 3 suggests that the MAE can be increased by alloying FePt with a material that decreases the band filling. A possible candidate is Mn, which has one electron less than Fe. The crystallographic structure and the magnetic phase diagram of $L1_0$ $Fe_{1-x}Mn_xPt$ alloys were investigated by Menshikov *et al.* in the whole concentration range.[40] In this alloy with competing exchange interactions, the magnetic order changes from the collinear ferromagnetic state of FePt, via canted ferromagnetic and antiferromagnetic states at intermediate concentrations, to the collinear antiferromagnetic state of MnPt. The arrangement of Fe and Mn on their sublattice is random, and only a small disorder between the Fe and the Pt sublattices is present. According to the magnetic phase diagram,[40] $Fe_{1-x}Mn_xPt$ should be ferromagnetic at room temperature and Mn concentrations less than about 20%. For our calculations we assumed a ferromagnetic order up 25% Mn, i.e., with the magnetic moments of all constituents aligned parallel to each other. From a CPA calculation for 25% Mn we find that the antiparallel alignment of the Mn spins with respect to Fe and Pt is lower in energy by a small amount, 2.1 mRy/atom. This is in agreement with the phase diagram[40] that in fact shows a nonferromagnetic order at low temperatures. We also note that the type of magnetic order can depend sensitively on the structural details, i.e., volume and c/a ratio, as well as compositional order. In Ref. 58, for example, the competition between ferromagnetic and antiferromagnetic order was studied for binary FePt. The authors found that ferromagnetism is stabilized relative to the antiferromagnetic state if the tetragonal distortion is decreased, i.e., if the c/a ratio is increased toward 1, or because of compositional disorder, which is always present in real samples. In a thin film, ferromagnetic order might be stabilized by interface/surface effects, or a modified c/a ratio or volume. A general analysis of the magnetic configuration in FePt and its alloys with Mn is, therefore, a quite complicated problem, which requires a separate investigation in itself.

In addition to the calculations for alloys with a randomly alloyed Fe-Mn sublattice, the situation that is encountered experimentally,[40] we calculated the MAE for two (hypothetical) ordered structures with Mn concentrations of 12.5% and 25%. These ordered alloys were modeled by two supercells, $2\times2\times1$ and $1\times1\times2$, in terms of the $L1_0$ unit cell, with one Mn atom located at the origin, retaining the fourfold symmetry in the basal plane of the $L1_0$ unit cell. For these supercells we considered both a parallel and an antiparallel alignment of the Mn spin with respect to the Fe and Pt spins. It was found that the parallel alignment is lower in energy by 7 mRy/f.u. for $x=0.125$, and 3 mRy/f.u. for $x=0.25$, respectively, supporting the chosen parallel alignment.

The position of the Fermi level of FePt with a reduced valence electron number for Fe by 0.50 and 0.25, corresponding to Mn concentrations of 50% and 25%, respectively, was estimated in a rigid-band approach and is marked by triangles in Fig. 3. Note that a strongly increased MAE can be expected by alloying FePt with Mn, but that a large degree of alloying decreases the MAE to lower values.

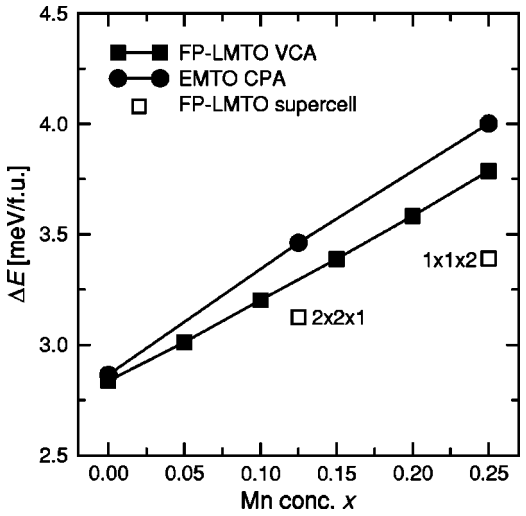

FIG. 4. Calculated MAE for $Fe_{1-x}Mn_xPt$ as a function of the Mn concentration x, obtained from FP-LMTO VCA and EMTO CPA calculations, as well as two FP-LMTO supercell calculations.

In Fig. 4 the calculated MAE of $Fe_{1-x}Mn_xPt$ is presented as a function of the Mn concentration x. The results, that are shown by closed squares, were obtained with the VCA. As can be seen in Fig. 4, the MAE increases monotonically with the Mn concentration x, i.e., when the effective charge on the Fe sublattice is reduced, as is expected from Fig. 3. For a Mn concentration of 25% the MAE is increased by 33% as compared to pure FePt. In order to verify the applicability of the VCA we performed EMTO CPA calculations as well. As can be seen from Fig. 4, the agreement between the CPA and the VCA results is satisfactory. Therefore, it can be concluded that the increased MAE of $Fe_{1-x}Mn_xPt$ is a band-filling effect. The MAE of the ordered structures modeled by supercells is lower than that of those with a randomly ordered Fe-Mn sublattice, but they are in reasonable agreement with the VCA and CPA results.

Since the origin of the altered MAE is band filling, the same effect might be expected by alloying FePt with Ir,[52] which has one electron less than Pt. Experimentally, however, it was found that the addition of Ir to FePt destroys the ferromagnetism.[59]

E. Magnetic moments of $Fe_{1-x}Mn_xPt$

For completeness, in Table II we list the spin and orbital magnetic moments as a function of the Mn concentration. The magnetic moment of FePt is 3.3 μ_B/f.u., which is partly due to an enhanced Fe magnetic moment and an induced magnetic moment on the Pt atom that is oriented parallel to that of the Fe sublattice, in agreement with the results of other authors.[17,26,42,44,45,60] The total spin magnetic moment increases with Mn concentration and is slightly larger in the FP-LMTO VCA calculations compared to the EMTO CPA

TABLE II. Spin and orbital moments from FP-LMTO supercell (SC) and EMTO CPA calculations.

Mn conc. x	total		Mn		Fe		Pt	
	SC	CPA	SC	CPA	SC	CPA	SC	CPA
			Spin moments (μ_B)					
0.0	3.242	3.233	-	-	2.923	2.937	0.3615	0.296
0.125	3.269	3.268	3.334	3.358	2.909	2.932	0.3363	0.282
0.25	3.269	3.302	3.255	3.364	2.894	2.928	0.3075	0.265
			Orbital moments (μ_B)					
0.0	0.115	0.122	-	-	0.069	0.078	0.045	0.043
0.125	0.082	0.110	0.031	0.043	0.070	0.078	0.040	0.037
0.25	0.086	0.099	0.034	0.046	0.068	0.077	0.030	0.029

results. Experimentally the magnetic moment was found to decrease with Mn concentration.[40] This was attributed by the authors to the coexistence of ferromagnetic and antiferromagnetic phases.

F. Dependence of MAE on c/a

For all calculations presented here a constant c/a ratio was assumed, since it only changes by 2% within the concentration range considered for $Fe_{1-x}Mn_xPt$.[40] In order to estimate the error in the MAE due to the imposed structure, the MAE of FePt as a function of the c/a ratio is shown in Fig. 5. The results are in good agreement with those by Sakuma.[44] If the c/a is decreased by 2% from the equilibrium value, which is the case at a Mn concentration of 25%,[40] the MAE decreases by 0.26 meV/f.u., or about 9% of the MAE of $Fe_{0.75}Mn_{0.25}Pt$. In a bulk FeMnPt alloy this would partly cancel the increase of the MAE with Mn concentration quoted above. However, in superlattices and nanoparticles, nonequilibrium c/a ratios can be stabilized and the strain dependence of the MAE might be used to tailor the MAE.[2–5] Figure 5 shows that a strong influence on the MAE is expected from a modification of the c/a ratio.

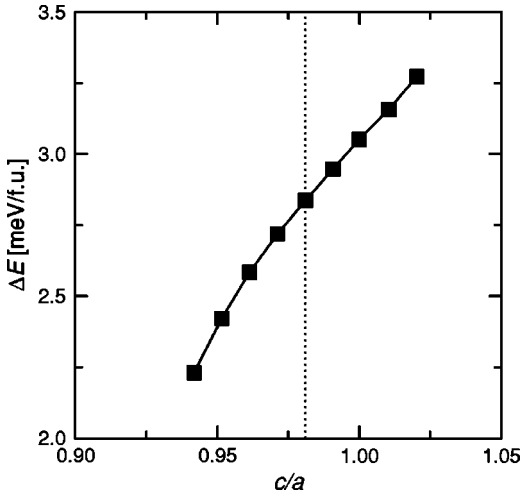

FIG. 5. Calculated MAE of FePt as a function of the c/a ratio of the $L1_0$ unit cell. The vertical dotted line indicates the experimental ratio, $c/a=0.981$. The calculations were done with the FP-LMTO method.

Experimental results concerning the MAE of (Fe,Mn)Pt thin films have only been published recently.[61] The MAE was observed to increase for a Mn concentration of 1% and was found to decrease for higher concentrations. This was attributed to the appearance of a (111) oriented phase in addition to the (001) phase at these concentrations.

IV. SUMMARY

The uniaxial MAE of $L1_0$ FePt and (Fe,Mn)Pt was studied from first principles using a FP-LMTO and an EMTO method. A projection to the different atomic types for the contribution to the MAE shows that Fe dominates (70% is found for this type). However, this does not mean that Pt is less important for the MAE. A calculation where the spin-orbit coupling is set to zero for Pt results in a MAE that is reduced by almost an order of magnitude. From this, one comes to a conclusion that—at first sight—is in contradiction to the information given by the atomic resolved MAE, namely, that it is the Pt atoms that are important. The analysis of Refs. 48 and 56 is consistent with both of these pieces of information, since it is shown that the large spin-orbit coupling in combination with strong hybridization is crucial.

The effect of noncomplete chemical order on the MAE was investigated within the CPA. It results in a strong dependence of the MAE on the degree of long-range chemical order and should therefore be taken into account in first-principles calculations in order to obtain a complete description of the MAE. The alloying of FePt with Mn on the Fe sublattice was treated by VCA and CPA. The MAE increases with the Mn concentration within the concentration range studied here—an effect that is attributed to band filling—and a good agreement between the VCA and the CPA was found. For a Mn concentration of 25% on the Fe sublattice, the MAE increases by 33%. Furthermore, a considerable enhancement of the MAE can be obtained if the c/a ratio is increased, e.g., by growing FePt as a superlattice in conjunction with other materials, or as part of nanocomposite materials.[2–6]

ACKNOWLEDGMENTS

Parts of the calculations were performed at the National Supercomputer Centre in Linköping (NSC), Sweden. Financial support from the Swedish Research Council (VR), the Swedish Foundation for Strategic Research (SSF), the Göran Gustafssson Foundation, and Seagate Research, Bloomington, is gratefully acknowledged. We thank Peter Oppeneer and Anna Delin for fruitful discussions.

*Electronic address: till.burkert@fysik.uu.se

[1] D. Weller, A. Moser, L. Folks, M. E. Best, W. Lee, M. Toney, M. Schwickert, J.-U. Thiele, and M. Doerner, IEEE Trans. Magn. **36**, 10 (2000).
[2] S. Sun, C. B. Murray, D. Weller, L. Folks, and A. Moser, Science **287**, 1989 (2000).
[3] H. Zeng, J. Li, J. P. Liu, Z. L. Wang, and S. Sun, Nature (London) **420**, 395 (2002).
[4] H. Zeng, R. Sabirianov, O. Mryasov, M. L. Yan, K. Cho, and D. J. Sellmyer, Phys. Rev. B **66**, 184425 (2002).
[5] J.-U. Thiele, S. Maat, and E. E. Fullerton, Appl. Phys. Lett. **82**, 2859 (2003).
[6] M. Ulmeanu, C. Antoniak, U. Wiedwald, M. Farle, Z. Frait, and S. Sun, Phys. Rev. B **69**, 054417 (2004).
[7] S. Mitani, K. Takanashi, M. Sano, H. Fujimori, A. Osawa, and H. Nakajima, J. Magn. Magn. Mater. **148**, 163 (1995).
[8] S. Okamoto, N. Kikuchi, O. Kitakami, T. Miyazaki, Y. Shimada, and K. Fukamichi, Phys. Rev. B **66**, 024413 (2002).
[9] R. F. C. Farrow, D. Weller, R. F. Marks, M. F. Toney, A. Cebollada, and G. R. Harp, J. Appl. Phys. **79**, 5967 (1996).
[10] M. Watanabe and M. Homma, Jpn. J. Appl. Phys., Part 1 **35**, L1264 (1996).
[11] J.-U. Thiele, L. Folks, M. F. Toney, and D. K. Weller, J. Appl. Phys. **84**, 5686 (1998).
[12] B. M. Lairson, M. R. Visokay, R. Sinclair, and B. M. Clemens, Appl. Phys. Lett. **62**, 639 (1993).
[13] J. Trygg, B. Johansson, O. Eriksson, and J. M. Wills, Phys. Rev. Lett. **75**, 2871 (1995).
[14] T. Burkert, O. Eriksson, P. James, S. I. Simak, B. Johansson, and L. Nordström, Phys. Rev. B **69**, 104426 (2004).
[15] M. Colarieti-Tosti, S. I. Simak, R. Ahuja, L. Nordström, O. Eriksson, D. Åberg, S. Edvardsson, and M. S. S. Brooks, Phys. Rev. Lett. **91**, 157201 (2003).
[16] R. Wu, C. Li, and A. J. Freeman, J. Magn. Magn. Mater. **99**, 71 (1991).
[17] G. H. O. Daalderop, P. J. Kelly, and M. F. H. Schuurmans, Phys. Rev. B **44**, R12054 (1991).
[18] G. H. O. Daalderop, P. J. Kelly, and M. F. H. Schuurmans, Phys. Rev. B **50**, 9989 (1994).
[19] O. Hjortstam, K. Baberschke, J. M. Wills, B. Johansson, and O. Eriksson, Phys. Rev. B **55**, 15 026 (1997).
[20] C. Uiberacker, J. Zabloudil, P. Weinberger, L. Szunyogh, and C. Sommers, Phys. Rev. Lett. **82**, 1289 (1999).
[21] H. J. F. Jansen, J. Appl. Phys. **67**, 4555 (1990).
[22] O. Eriksson, M. S. S. Brooks, and B. Johansson, Phys. Rev. B **41**, R7311 (1990).
[23] O. Eriksson, B. Johansson, R. C. Albers, A. M. Boring, and M. S. S. Brooks, Phys. Rev. B **42**, R2707 (1990).
[24] Y. Wu, J. Stöhr, B. D. Hermsmeier, M. G. Samant, and D. Weller, Phys. Rev. Lett. **69**, 2307 (1992).
[25] P. Söderlind, O. Eriksson, B. Johansson, R. C. Albers, and A. M. Boring, Phys. Rev. B **45**, 12 911 (1992).
[26] P. Ravindran, A. Kjekshus, H. Fjellvaag, P. James, L. Nordström, B. Johansson, and O. Eriksson, Phys. Rev. B **63**, 144409 (2001).
[27] V. I.Anisimov, J. Zaanen, and O. K. Andersen, Phys. Rev. B **44**, 943 (1991).
[28] O. K. Andersen, Phys. Rev. B **12**, 3060 (1975).
[29] H. L. Skriver, *The LMTO Method: Muffin-Tin Orbitals and Electronic Structure* (Springer, Berlin, 1984).
[30] J. M. Wills, O. Eriksson, M. Alouani, and D. L. Price, in *Electronic Structure and Physical Properties of Solids: The Uses of the LMTO Method* (Springer, Berlin, 2000), pp. 148–167.
[31] M. Weinert, R. E. Watson, and J. W. Davenport, Phys. Rev. B **32**, 2115 (1985).
[32] G. H. O. Daalderop, P. J. Kelly, and M. F. H. Schuurmans, Phys. Rev. B **41**, 11 919 (1990).
[33] P. E. Blöchl, O. Jepsen, and O. K. Andersen, Phys. Rev. B **49**, 16 223 (1994).
[34] H. J. Monkhorst and J. D. Pack, Phys. Rev. B **13**, 5188 (1976).
[35] S. Froyen, Phys. Rev. B **39**, 3168 (1989).
[36] M. Methfessel and A. T. Paxton, Phys. Rev. B **40**, 3616 (1989).
[37] O. Grotheer and M. Fähnle, Phys. Rev. B **58**, 13 459 (1998).
[38] L. V. Pourovskii, A. V. Ruban, L. Vitos, H. Ebert, B. Johansson, and I. A. Abrikosov, Phys. Rev. B **71**, 094415 (2005).
[39] L. Vitos, Phys. Rev. B **64**, 014107 (2001).
[40] A. Z. Menshikov, V. P. Antropov, G. P. Gasnikova, Y. A. Dorofeyev, and V. A. Kazantsev, J. Magn. Magn. Mater. **65**, 159 (1987).
[41] P. Villars and L. D. Calvert, eds., *Pearson's Handbook of Crystallographic Data for Intermetallic Phases* (American Society for Metals, Metals Park, OH, 1985).
[42] A. B. Shick and O. N. Mryasov, Phys. Rev. B **67**, 172407 (2003).
[43] P. M. Oppeneer, J. Magn. Magn. Mater. **188**, 275 (1998).
[44] A. Sakuma, J. Phys. Soc. Jpn. **63**, 3053 (1994).
[45] I. Galanakis, M. Alouani, and H. Dreyssé, Phys. Rev. B **62**, 6475 (2000).
[46] J. B. Staunton, S. Ostanin, S. S. A. Razee, B. Gyorffy, and L. Szunyogh, J. Phys.: Condens. Matter **16**, S5623 (2004).
[47] S. Ostanin, S. S. A. Razee, J. B. Staunton, B. Ginatempo, and E. Bruno, J. Appl. Phys. **93**, 453 (2003).
[48] I. V. Solovyev, P. H. Dederichs, and I. Mertig, Phys. Rev. B **52**, 13 419 (1995).
[49] O. A. Ivanov, L. V. Solina, V. A. Demshina, and L. M. Magat, Phys. Met. Metallogr. **35**, 92 (1973).
[50] J. Yu, U. Ruediger, A. D. Kent, R. F. C. Farrow, R. F. Marks, D. Weller, L. Folks, and S. S. P. Parkin, J. Appl. Phys. **87**, 6854 (2000).
[51] H. Kanazawa, G. Lauhoff, and T. Suzuki, J. Appl. Phys. **87**, 6143 (2000).
[52] J. B. Staunton, S. Ostanin, S. S. A. Razee, B. L. Gyorffy, L. Szunyogh, B. Ginatempo, and E. Bruno, Phys. Rev. Lett. **93**, 257204 (2004).

[53] A. Cebollada, D. Weller, J. Sticht, G. R. Harp, R. F. C. Farrow, R. F. Marks, R. Savoy, and J. C. Scott, Phys. Rev. B **50**, 3419 (1994).
[54] M. M. Schwickert, K. A. Hannibal, M. F. Toney, M. Best, L. Folks, J.-U. Thiele, A. J. Kellock, and D. Weller, J. Appl. Phys. **87**, 6956 (2000).
[55] L. Nordström, M. S. S. Brooks, and B. Johansson, J. Phys.: Condens. Matter **4**, 3261 (1992).
[56] I. Galanakis, P. M. Oppeneer, P. Ravindran, L. Nordström, P. James, M. Alouani, H. Dreysseé, and O. Eriksson, Phys. Rev. B **63**, 172405 (2001).
[57] P. Bruno, Phys. Rev. B **39**, R865 (1989).
[58] G. Brown, B. Kraczek, A. Janotti, T. C. Schulthess, G. M. Stocks, and D. D. Johnson, Phys. Rev. B **68**, 052405 (2003).
[59] T. Goto, J. Takahashi, M. Nakamura, T. Hirose, K. Watanabe, and H. Yoshida, J. Magn. Magn. Mater. **226-230**, 1656 (2001).
[60] T. Koide, T. Shidara, K. Yamaguchi, A. Fujimori, H. Fukutani, N. Nakajima, T. Sugimoto, T. Katayama, and Y. Suzuki, Phys. Rev. B **53**, 8219 (1996).
[61] J. C. A. Huang, Y. C. Chang, C. C. Yu, Y. D. Yao, Y. M. Hu, and C. M. Fu, J. Appl. Phys. **93**, 8173 (2003).